

Vertically divergent responses of SOC decomposition to soil moisture in a changing climate

Marleen Pallandt^{1,2}, Bernhard Ahrens¹, Sujan Koirala¹, Markus Reichstein^{1,2}, Holger Lange³, Marion Schrumpf^{1,2}, Sönke Zaehle^{1,2}

¹ Max Planck Institute for Biogeochemistry, Hans-Knöll Str. 10, 07745 Jena, Germany

² International Max Planck Research School (IMPRS) for Global Biogeochemical Cycles, Hans-Knöll Str. 10, 07745 Jena, Germany

³ Norwegian Institute of Bioeconomy Research, Høgskoleveien 8, 1433 Ås, Norway

Contents of this file

Text S1: Comparison of DAMM model to observations at multiple depths

Figure S1: Conceptual graph for changes in Michaelis-Menten terms

Figure S2: SOC content from SoilGrids

Figure S3: Temperature- and moisture driven changes in modelled decomposition rates

Figure S4: Model mean historic soil moisture and soil moisture changes by the end of the century

Figure S5: Moisture driven changes in modelled decomposition rates

Figure S6: Comparison of different DAMM model runs to observations at different soil midpoint depths (cm)

Figure S7: Sensitivity of model results to different initial substrate concentrations

Figure S8: Sensitivity of model results to declining oxygen gradient

Table S1: Parameter values and constants used in this study

Table S2: CMIP5 models used in this study

Introduction

This supporting information file includes a conceptual visualization of the DAMM model (Fig. S1); parameters of the DAMM model used in this study (Table S1); a map of SOC content from SoilGrids at multiple depths (Fig. S2); CMIP5 mean historic soil moisture and mean soil moisture changes between the historic and RCP8.5 simulation period (Fig. S4); sensitivity of DAMM model to different total substrate concentrations ($S_{x,total}$) and an absolute change in water content between the historic and RCP8.5 simulation period; and model results similar to Figs. 1 and 2 for the additional CMIP5 models in this study (Figs. S3 and S5, Table S2). All methods and data used to produce these figures and tables are described under "Data and Methods" (Section 2) of the main manuscript. R-code to run the DAMM model with CMIP5 data can be downloaded from https://git.bgc-jena.mpg.de/mpalla/pallandt_et al2020_jgrbg_decomposition_sm_response.git.

This supporting information file further includes a comparison of the DAMM model to site level observations from Hicks Pries et al. (2017) at multiple soil depth intervals to 1 m (Text S1 and Fig. S6). The methods and results are described in detail in the supporting information as they support, but are not essential to, the main manuscript. The data were downloaded with the original manuscript as provided by Hicks Pries et al. (2017).

Text S1. Comparison of DAMM model to observations at multiple depths

Methodology

Hicks Pries et al. (2017) measured soil C flux ($\text{g C m}^{-3} \text{h}^{-1}$), soil temperature, soil moisture at the five following mid-point depths: 7.5, 22.5, 40, 60, 80 cm. Soil C properties were measured at 10 cm depth intervals from 0 – 100 cm. Gomez et al. (2002) measured porosity at 15 cm depth intervals from 0– 45 cm. Similar to Section 2.3, soil C stocks were recalculated to densities (g C cm^{-3}) and together with soil porosity calculated as a weighted average for each layer at the 5 midpoint depths. The DAMM model was ran thrice: 1) Standard DAMM model run, using the measured SM, soil temperature, porosity and soil C content as inputs for each depth interval; 2) As the standard model run, but using a fixed soil C content (calculated as the mean measured soil C content between 0 – 100 cm) for each soil layer, to test how sensitive the model is to changes in substrate availability; 3) As the standard model run, but with a linearly declining value for the oxygen fraction in air ($O_{2,airfrac}$ from 0.21 to 0.04 between 0 and 100 cm soil depth, to test the sensitivity of the model to a reduced oxygen gradient in the deeper soil. Reported measurements of oxygen concentrations at multiple depth intervals up to 100 cm depth are rare, and values vary highly with soil type, soil moisture content and time of measurement (Hu & Linnartz, 1972; Runkles, 1956; Silver et al., 1999). Our back of the envelope calculation, using a minimum value of 0.04, is based on some of the reported lower values. The parameter α_{Sx} , which describes the base respiration at the site, was

refitted using the 'modFit' function of the R package FME (methods "L-BFGS-B" and "Marq" to avoid local minima) by minimizing the residuals between the observed soil CO₂ fluxes and the values predicted by the DAMM model. DAMM model parameters $E_{a_{S_x}}$, kM_{S_x} , kM_{O_2} , and all constants (Table S1) were not refitted, but remained the same as in our application of the DAMM model on the CMIP5 data (values taken directly from Davidson et al. (2012)). All analyses were done in RStudio (RStudio Team, 2018) using packages ModelMetrics and FME).

Results

When running the DAMM model with the same parameters as listed in Table S1, only refitting parameter α_{S_x} , the model captures the observed fluxes relatively well (Fig. S6), with an R^2 of 0.52 and RMSE of 0.19. At lower depths, the model slightly overestimates the observed fluxes, but these are generally very small (close to zero). The model is very sensitive to changes in substrate availability: When using a constant value for C density (calculated as the mean C density between 0 and 100 cm depth), the DAMM model was no longer able to capture the observed fluxes at any given depth (Fig S6, $R^2 = 0$, RMSE is 0.27). The model was not at all sensitive to changes in the oxygen fraction in air ($O_{2,airfrac}$ declining from 0.21 to 0.04), or other estimates of the half saturation constant for oxygen: Both model runs had the same rounded R^2 (0.58) and RMSE (0.18) as for the standard model run. Therefore, from this simple site-level exercise we can see that DAMM is capable of modeling the CO₂ efflux throughout the soil profile relatively well, and that substrate availability dominates the modeled response. A smaller role of the oxygen term at this site is in line with our expectations, as the soil seems to be well drained most of the time: The soil porosity at this site is high (0.62), but the maximum observed soil moisture is only 0.38. We did not find observations for this site's soil porosity below 45 cm depth, but it is likely that porosity further declined with soil depth with lower SOC content and compaction (Maier et al., 2010). The slight overestimation of modeled fluxes from the two deepest soil layers might be related to uncertain estimates of the available C substrate. A deep analysis of the specific causes, however, falls outside of the scope of this paper.

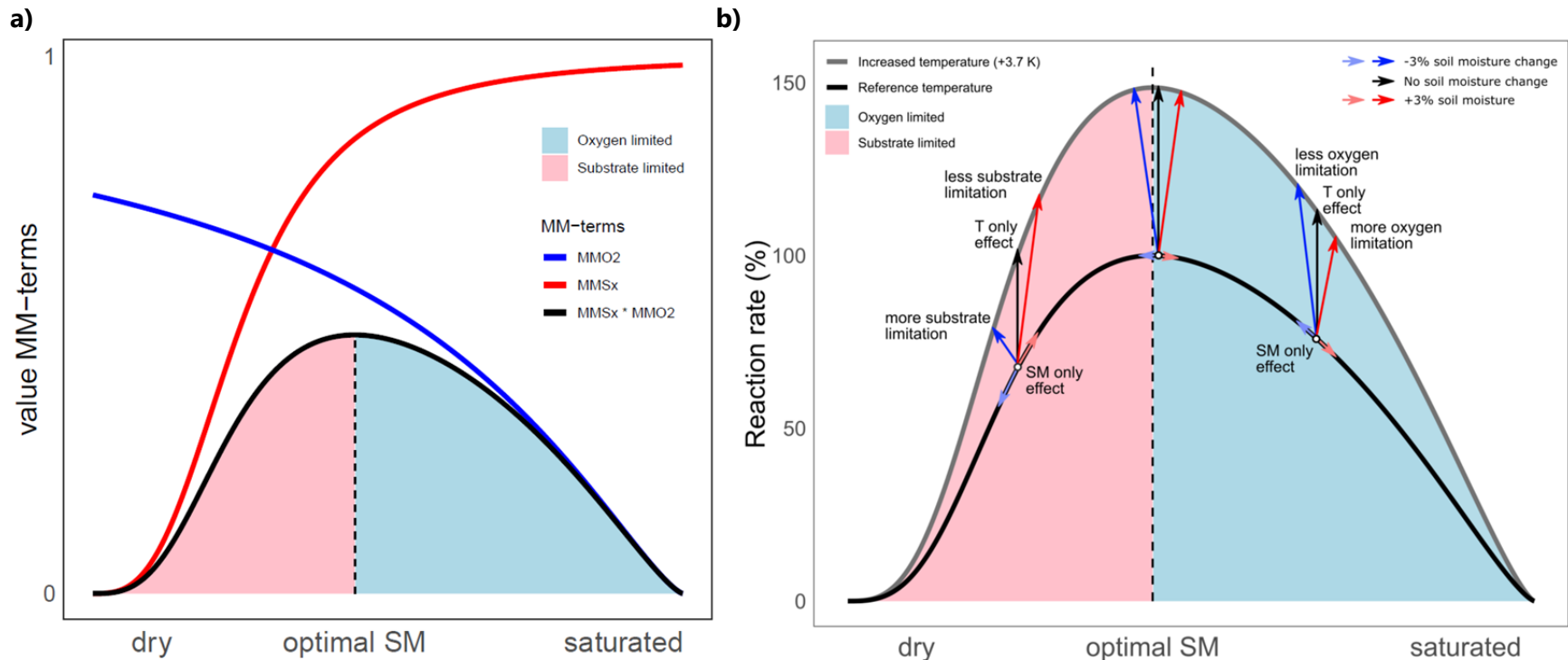


Figure S1. Conceptual visualizations of the DAMM model. **a)** Change in Michaelis-Menten (MM) terms in response to soil moisture (SM). In a dry soil, substrate availability (MMSx, red line) increases with increases in soil moisture. As the soil gets wetter and more saturated, oxygen availability (MMO2, blue line) declines. The combined SM effect (MMSx * MMO2, black line) is a gradual, non-symmetrical change from a substrate limited domain (pink shade) into an oxygen-limited domain (light blue shade) as a soil becomes wetter. At optimal SM (dotted line), the SM-effect is at its maximum rate. **b)** Change in reaction rate (%) in response to SM changes at reference temperature (Table S1: $T_{ref} = 283.15$ °K, black line) and increased temperature (+3.7 °K, grey line). Arrows indicate the change in reaction rate when soil moisture does not change (T only, black arrows), decreases by 3% (blue arrows), or increases by 3% (red arrows). The light blue and red arrows indicate the SM only change (no temperature change) to a 3% decrease/increase in SM, respectively. Around optimal SM (dotted line), temperature changes dominate the change in the reaction rate.

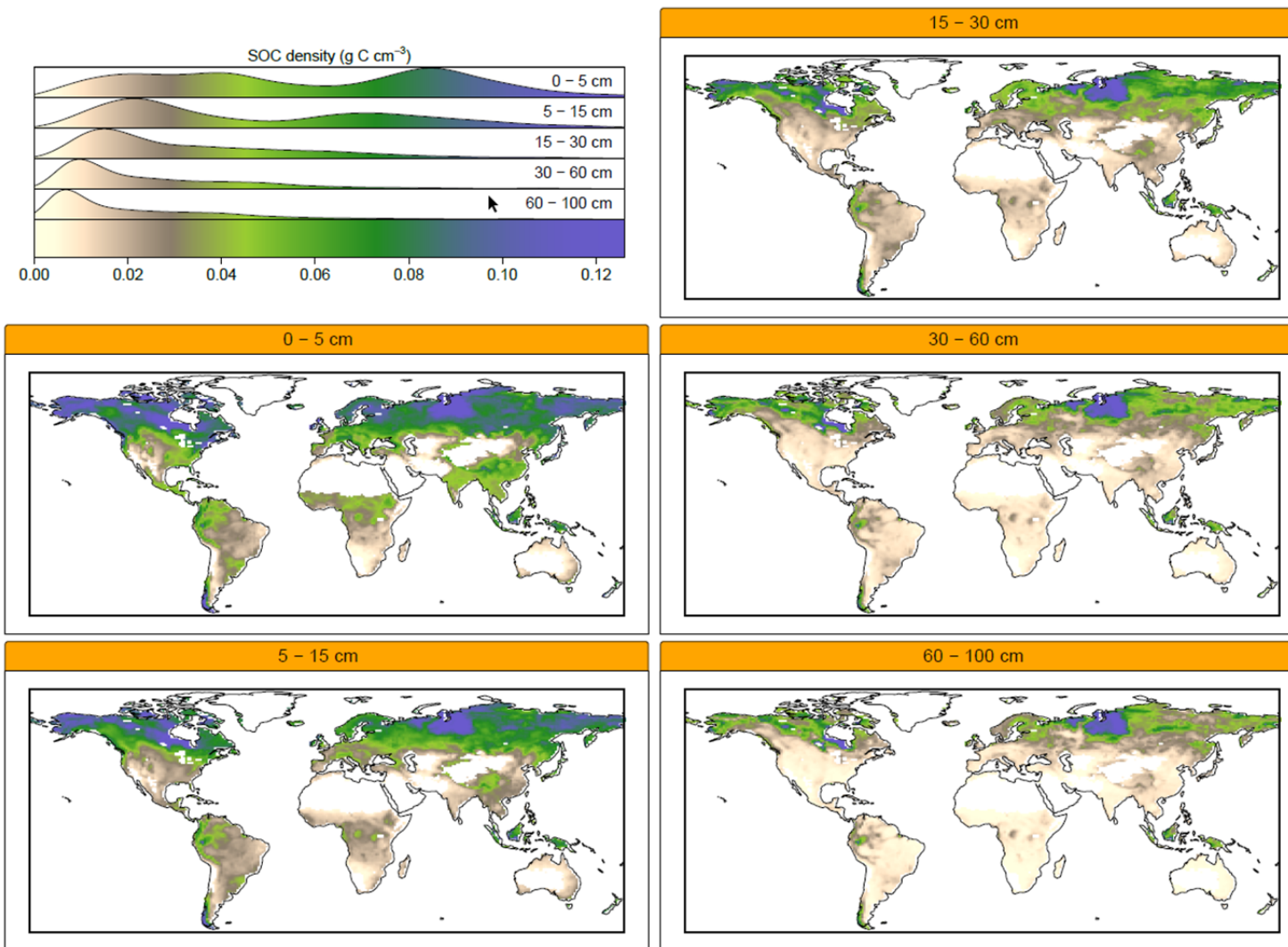


Figure S2. Soil organic carbon (SOC) content ($S_{x,tot}$, Eq. 4) in g C cm^{-3} from SoilGrids. Five depths until 1m are shown, at the spatial resolution of MCIP5 model CESM1-BGC.

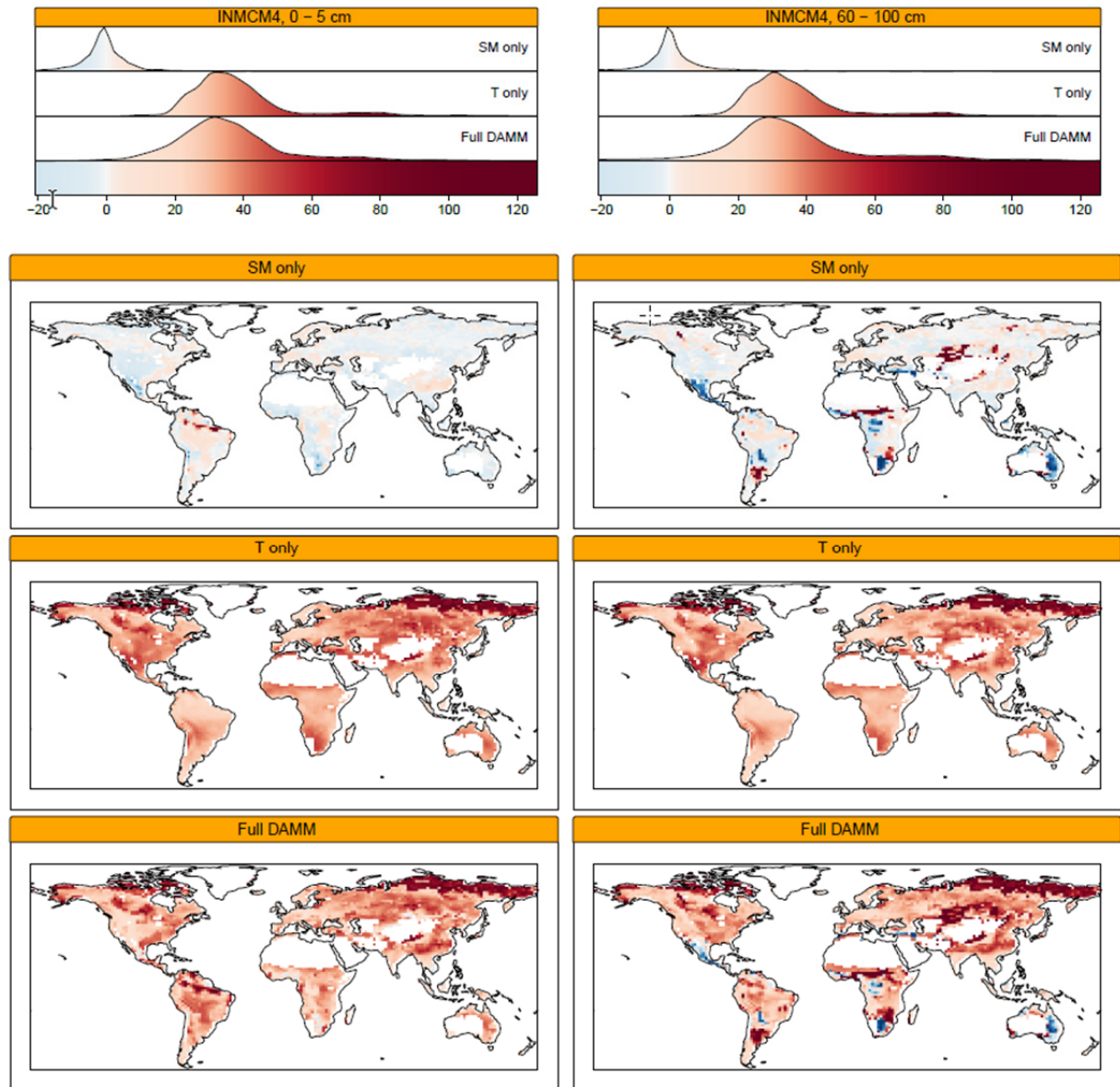


Figure S3a. Changes in modelled decomposition rates in top- and bottom soil layers for CMIP5 model INM-CM4, due to soil moisture changes (SM only); due to temperature changes (T-only); due to soil moisture and temperature changes (Full DAMM). Breaks and colors same as Fig. 1.

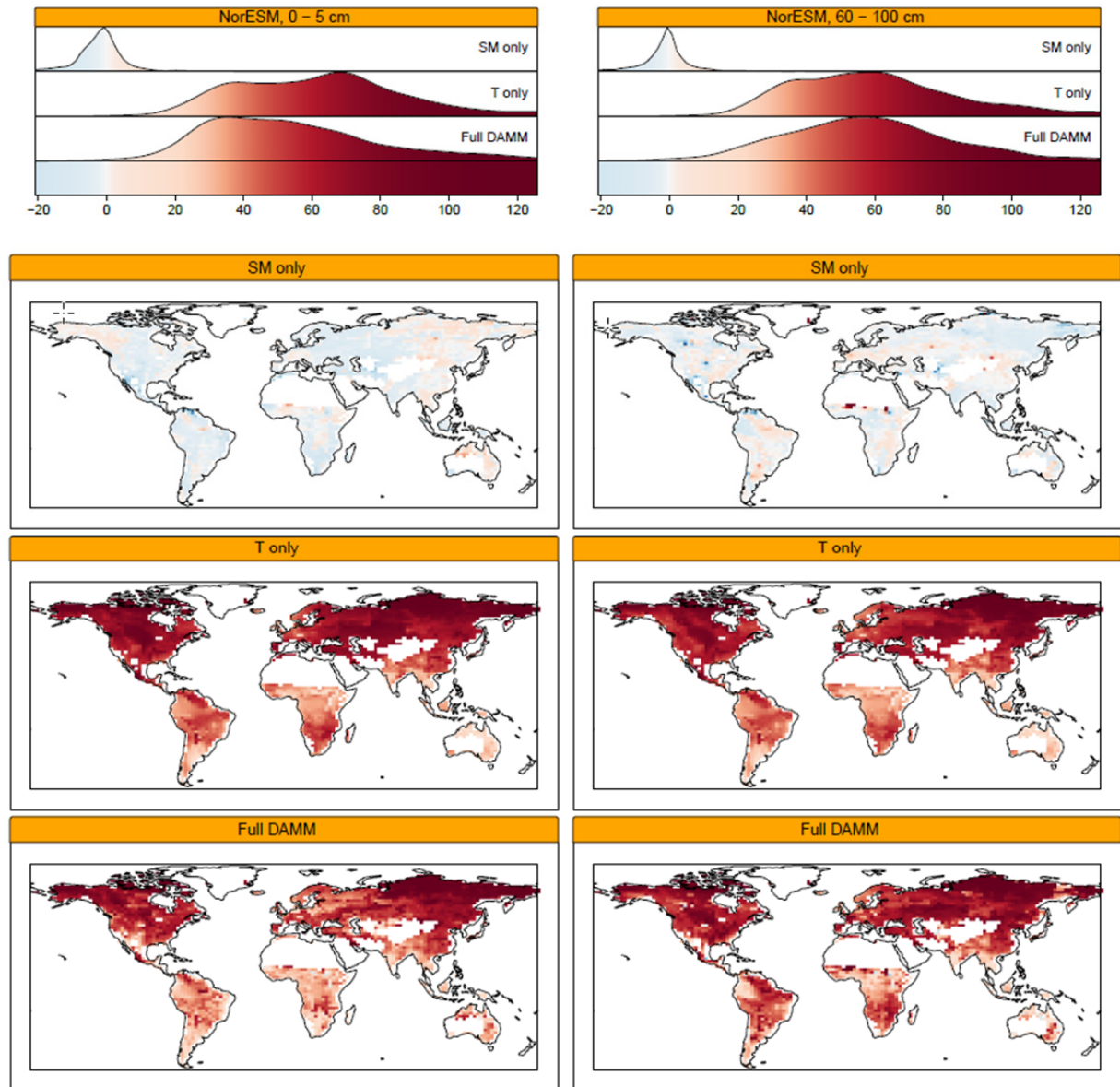


Figure S3b. Changes in modelled decomposition rates in top- and bottom soil layers for CMIP5 model NorESM-1M, due to soil moisture changes (SM only); due to temperature changes (T-only); due to soil moisture and temperature changes (Full DAMM). Breaks and colors same as Fig. 1.

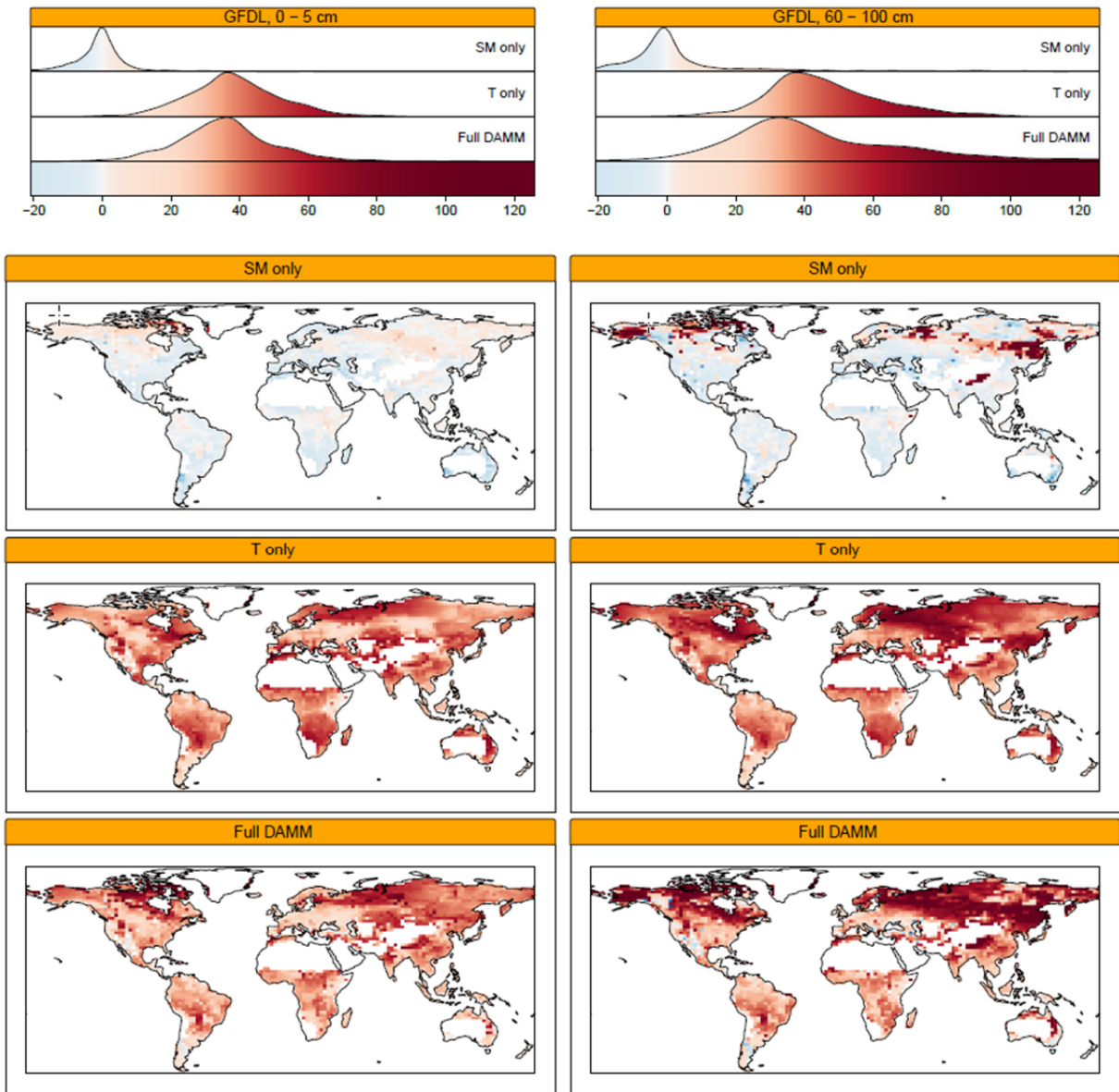


Figure S3c. Changes in modelled decomposition rates in top- and bottom soil layers for CMIP5 model GFDL-ESM2M, due to soil moisture changes (SM only); due to temperature changes (T-only); due to soil moisture and temperature changes (Full DAMM). Breaks and colors same as Fig. 1.

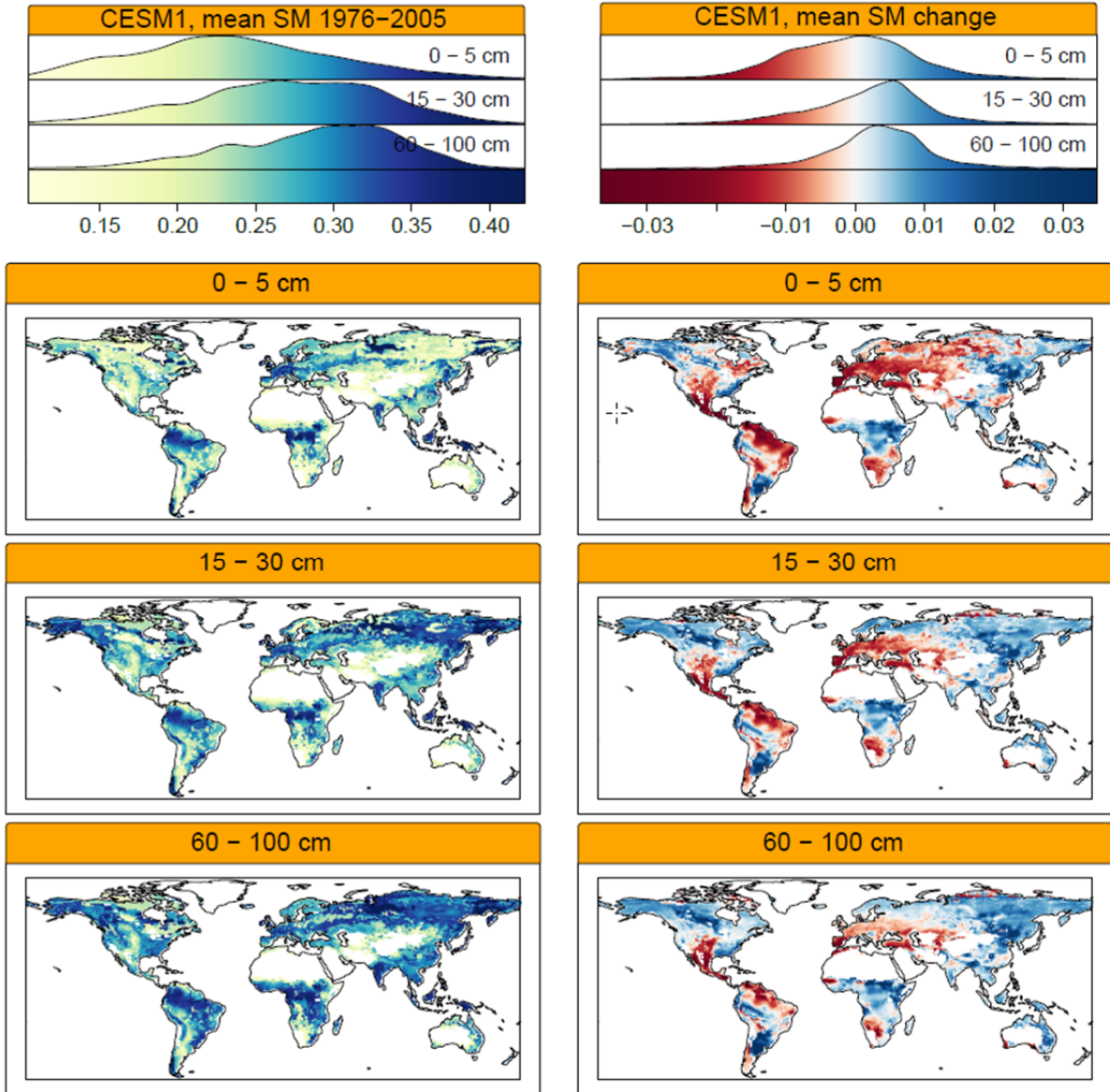


Figure S4a. Mean soil moisture (\overline{SM}) for historic period (1976–2005) and mean soil moisture differences ($\Delta\overline{SM}$) between historic and RCP8.5 (2070–2099) simulation period, for CESM1-BGC.

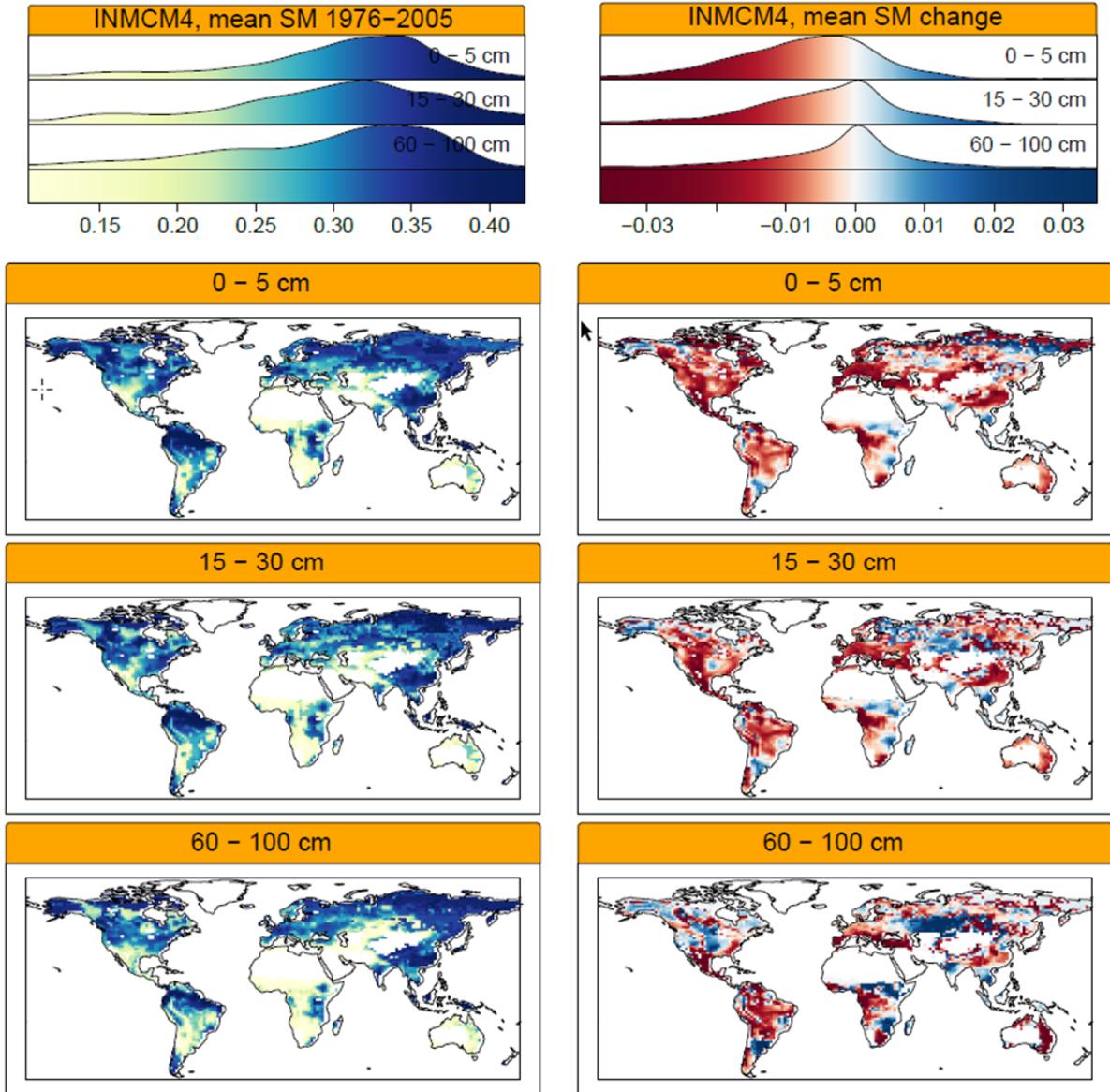


Figure S4b. Mean soil moisture (\overline{SM}) for historic period (1976–2005) and mean soil moisture differences ($\Delta\overline{SM}$) between historic and RCP8.5 (2070–2099) simulation period, for INM-CM4.

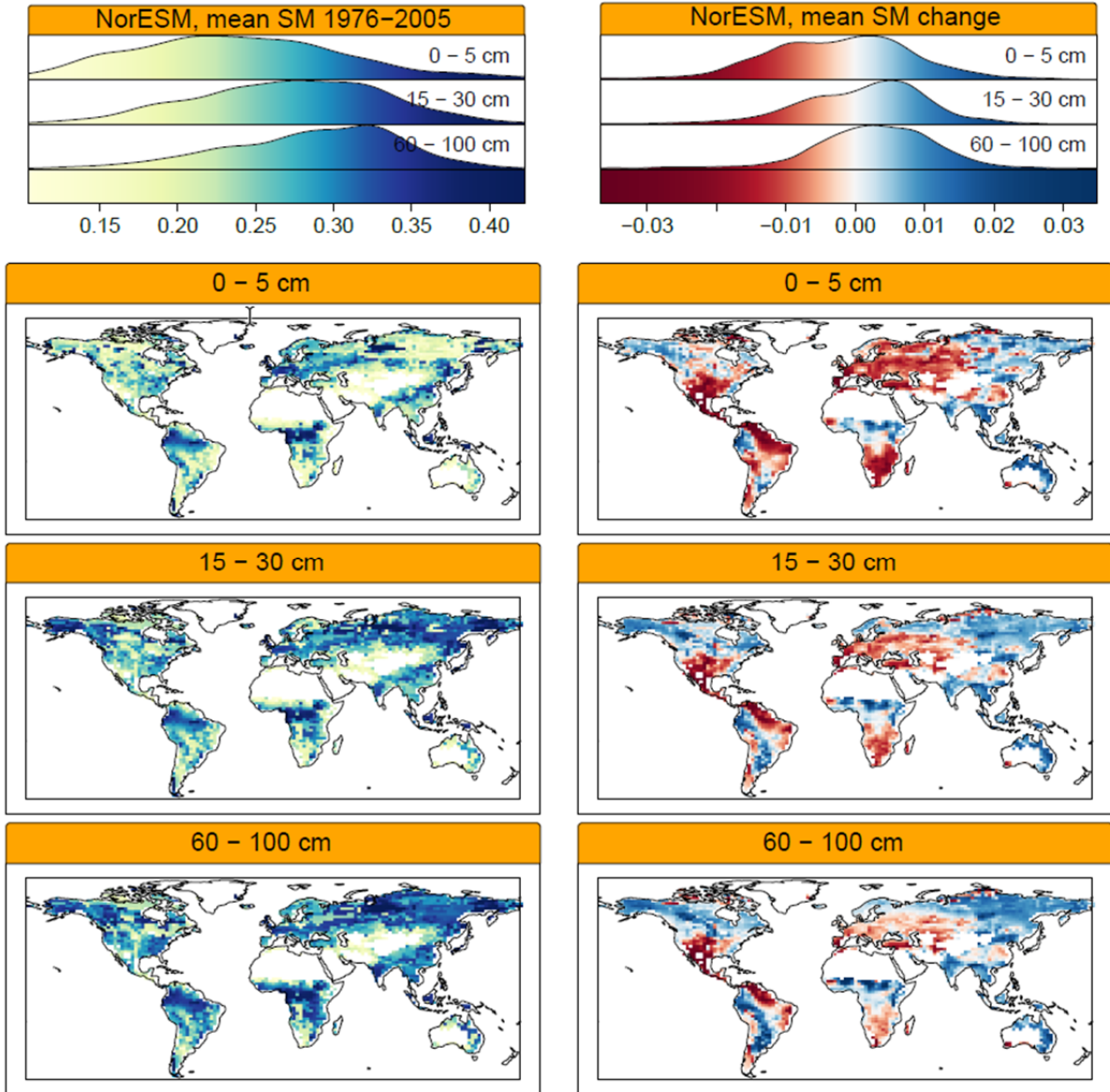


Figure S4c. Mean soil moisture (\overline{SM}) for historic period (1976–2005) and mean soil moisture differences ($\Delta\overline{SM}$) between historic and RCP8.5 (2070–2099) simulation period, for NorESM-1M.

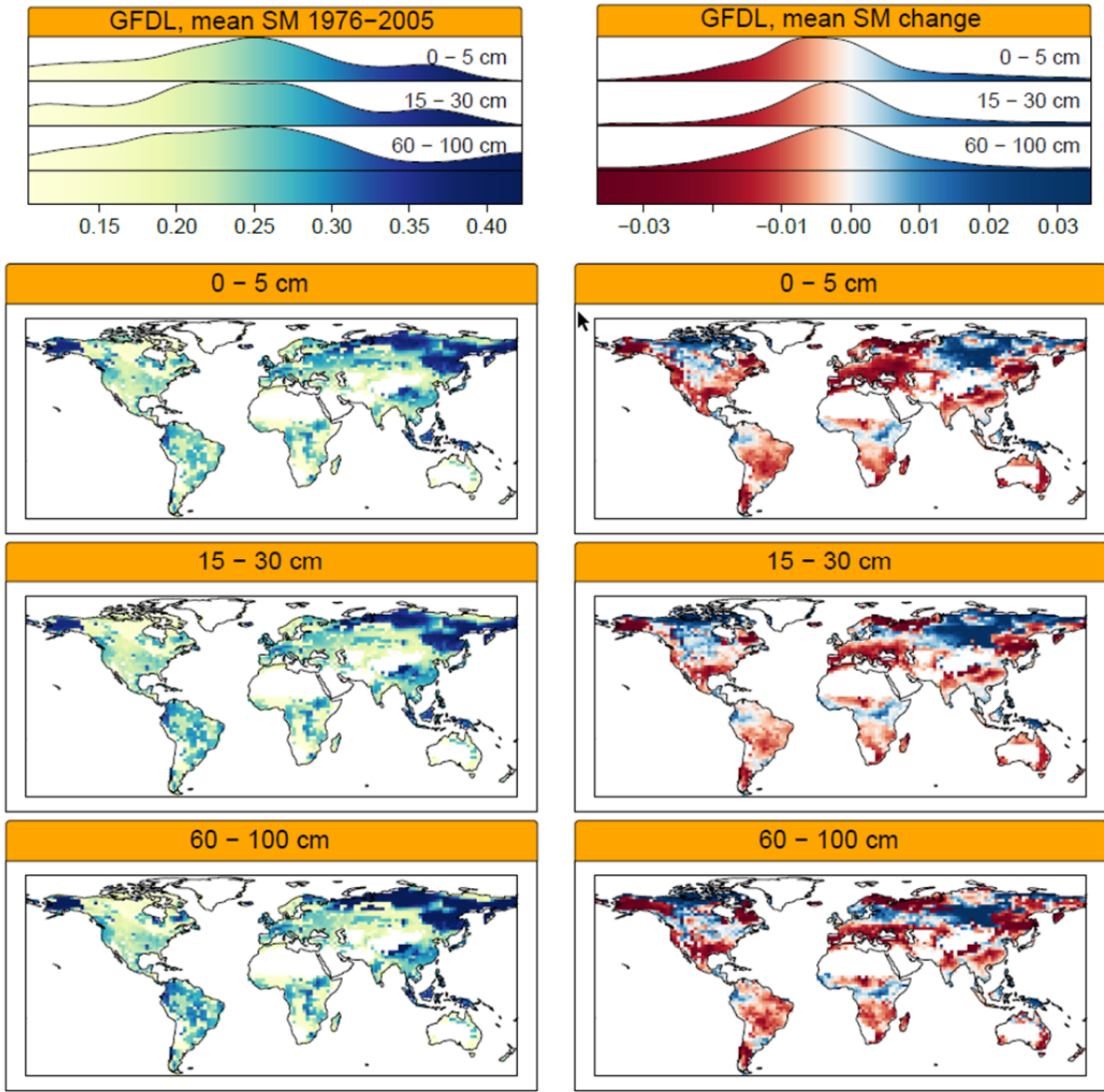


Figure S4d. Mean soil moisture (\overline{SM}) for historic period (1976–2005) and mean soil moisture differences ($\Delta\overline{SM}$) between historic and RCP8.5 (2070–2099) simulation period, for GFDL-ESM2M.

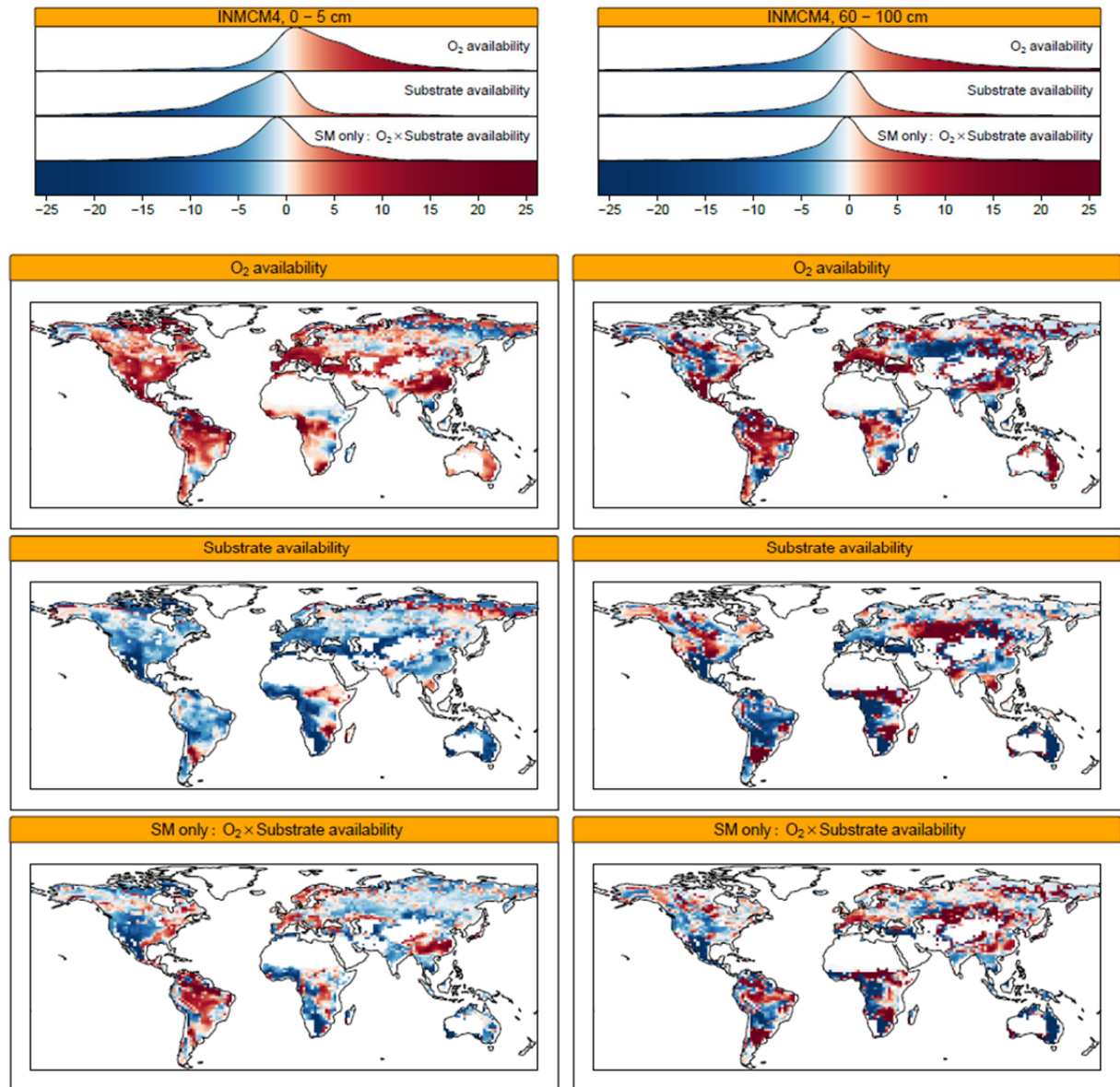


Figure S5a. Changes in modelled decomposition rates in top- and bottom soil layers for INM-CM4, due to changes in oxygen availability (top panel); due to changes in substrate availability (middle panel); and the combined soil moisture effect (SM only: $O_2 \times$ Substrate availability, bottom panel). Breaks and colors same as Fig. 2.

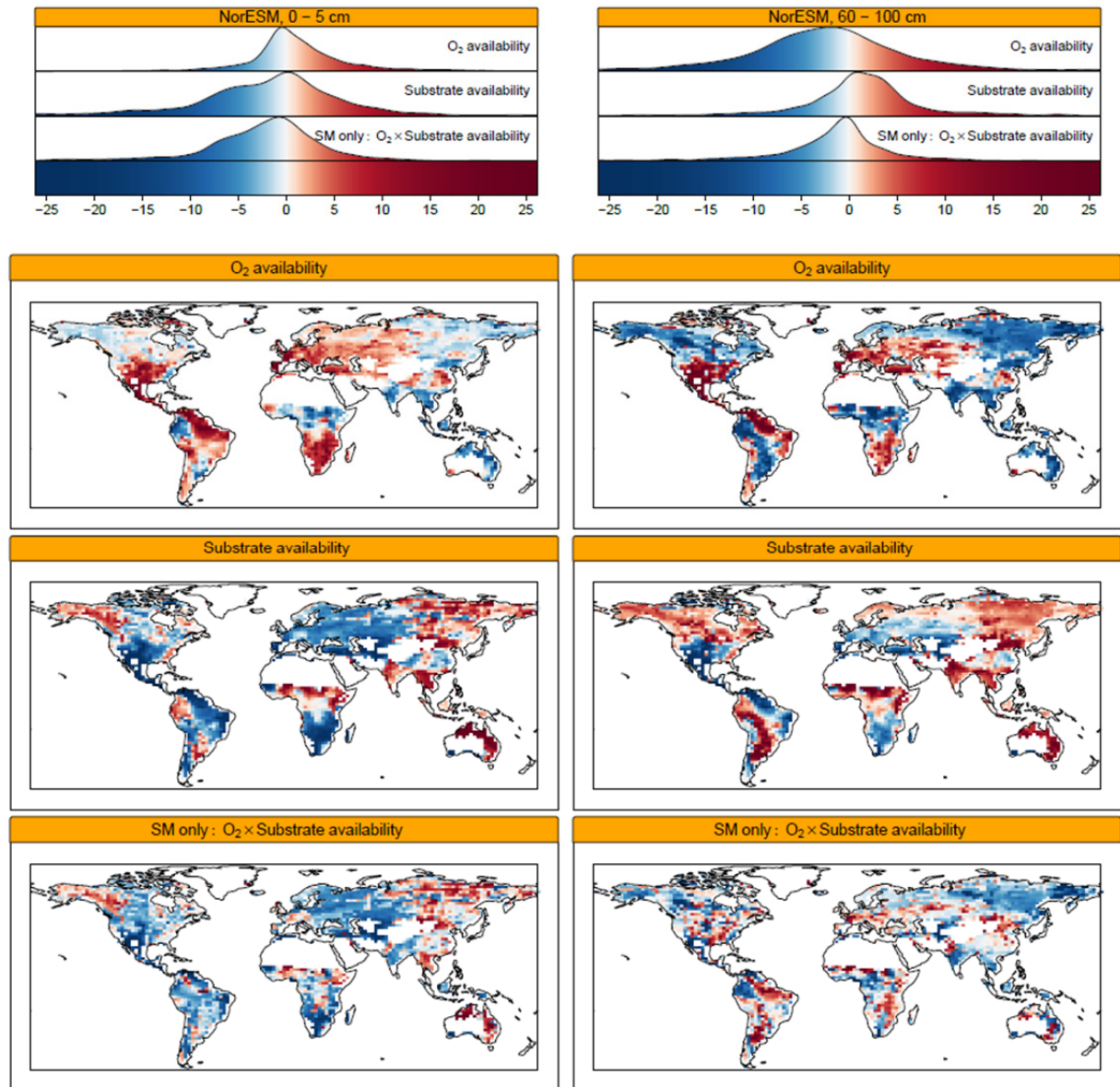


Figure S5b. Changes in modelled decomposition rates in top- and bottom soil layers for NorESM-1M, due to changes in oxygen availability (top panel); due to changes in substrate availability (middle panel); and the combined soil moisture effect (SM only: O₂ × Substrate availability, bottom panel). Breaks and colors same as Fig. 2.

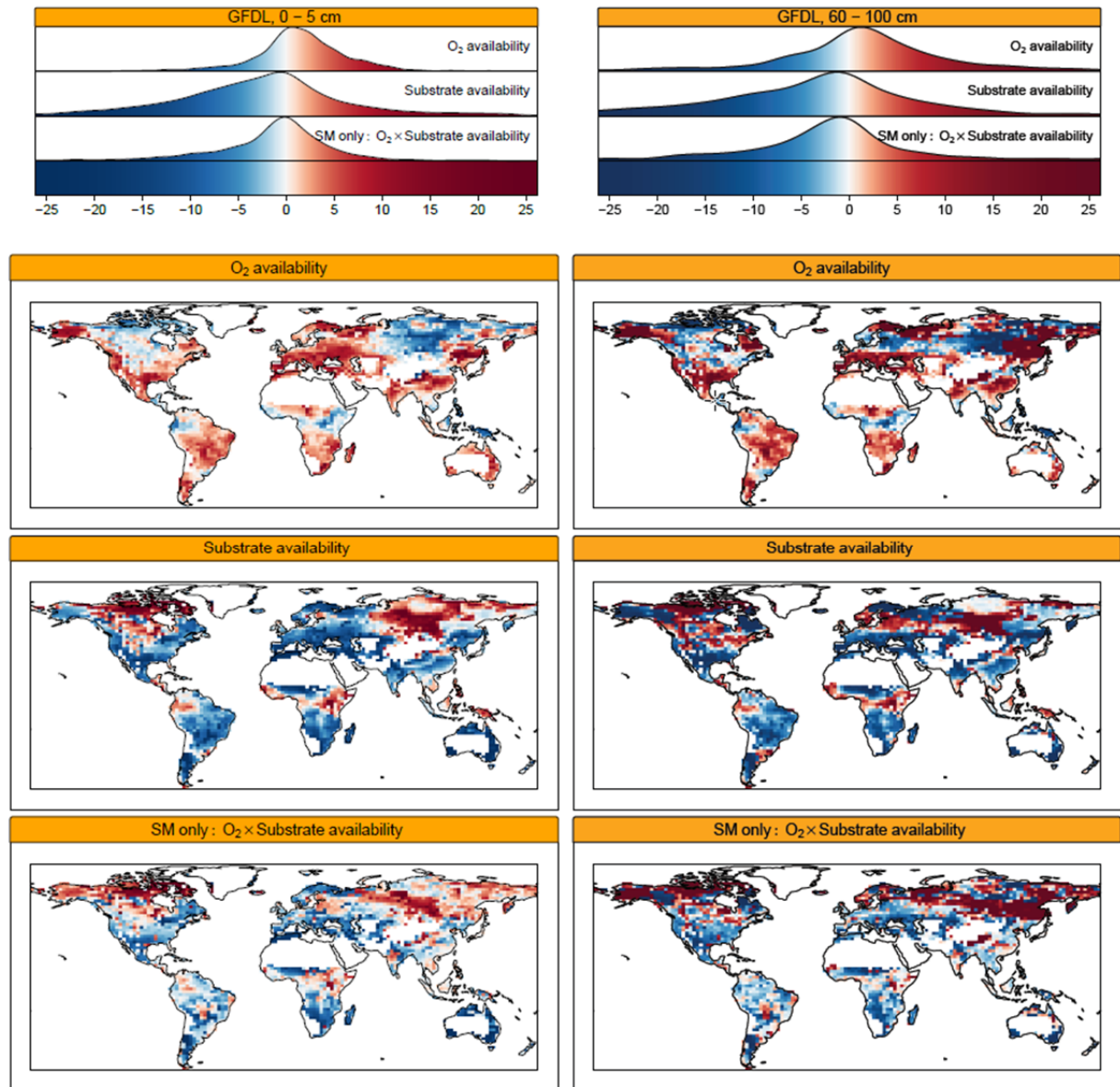


Figure S5c. Changes in modelled decomposition rates in top- and bottom soil layers for GFDL-ESM2M, due to changes in oxygen availability (top panel); due to changes in substrate availability (middle panel); and the combined soil moisture effect (SM only: $O_2 \times$ Substrate availability, bottom panel). Breaks and colors same as Fig. 2.

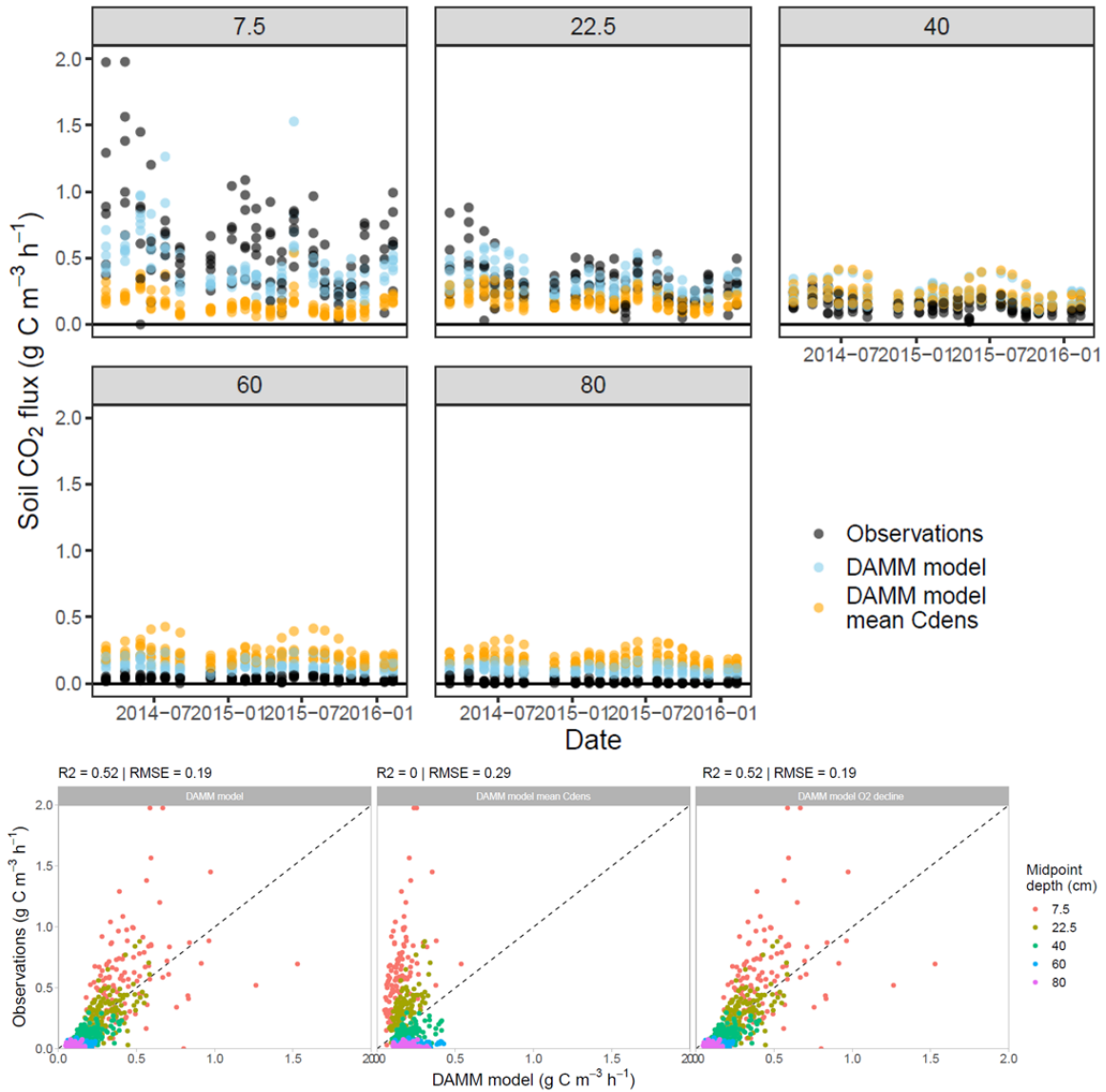


Figure S6. Comparison of different DAMM model runs to observations at different soil midpoint depths (cm). The top panel shows a time series with the observations (black points), the DAMM model run using measured C densities for each soil layer (DAMM model, blue points) and the DAMM model run using a constant C density for each soil layer (DAMM model mean Cdens, orange points). For figure clarity, the DAMM model run with declining oxygen (DAMM model O₂ decline) is not shown in the upper panel as the data points overlay with the standard model run. The bottom panel shows the goodness of fit between observations and all three DAMM model runs: DAMM model (using measured C densities per soil layer), DAMM model mean Cdens (using a constant mean C density per soil layer), and DAMM model O₂ decline (using a linearly declining O₂ gradient per soil layer). Points are colored by soil midpoint depth.

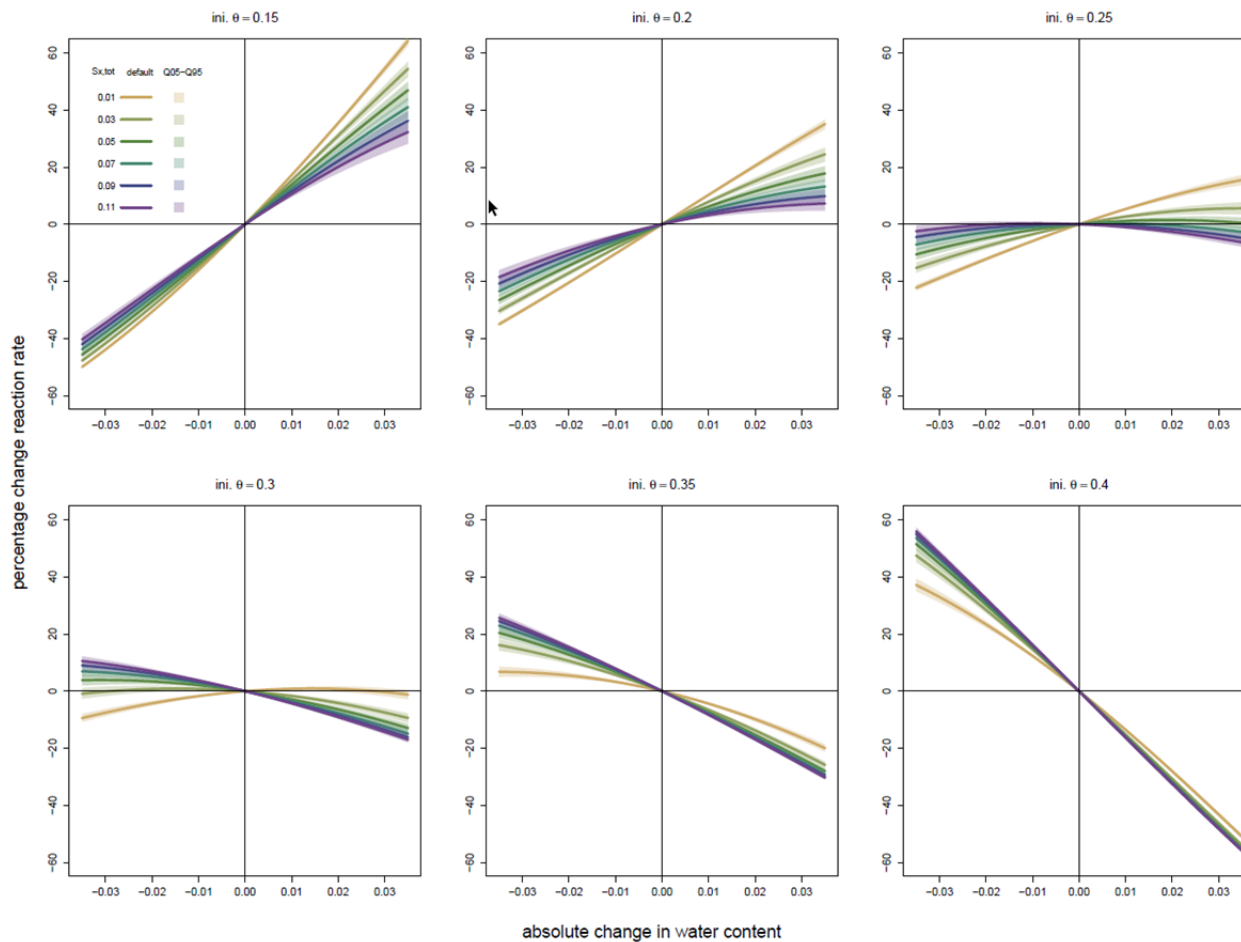


Figure S7. Sensitivity of DAMM model "SM only" to different total substrate concentrations ($S_{x,total}$) and an absolute change in water content between the historic and RCP8.5 simulation period. Similar to Fig. 3, divergence in the reaction rate due to the initial soil moisture conditions is visible as initial soil moisture content (init. θ) increases from 0.15 to 0.4 in each sub panel. Shading represents the sensitivity range (Q05 – Q95: 5th – 95th percentile) to $\pm 20\%$ changes in the DAMM parameters used in this study (α_{S_x} , Ea_{S_x} , kM_{S_x} and kM_{O_2} , Table S1). CMIP5 models' historic mean soil moisture ranges from 0.24 – 0.29 (Table S2).

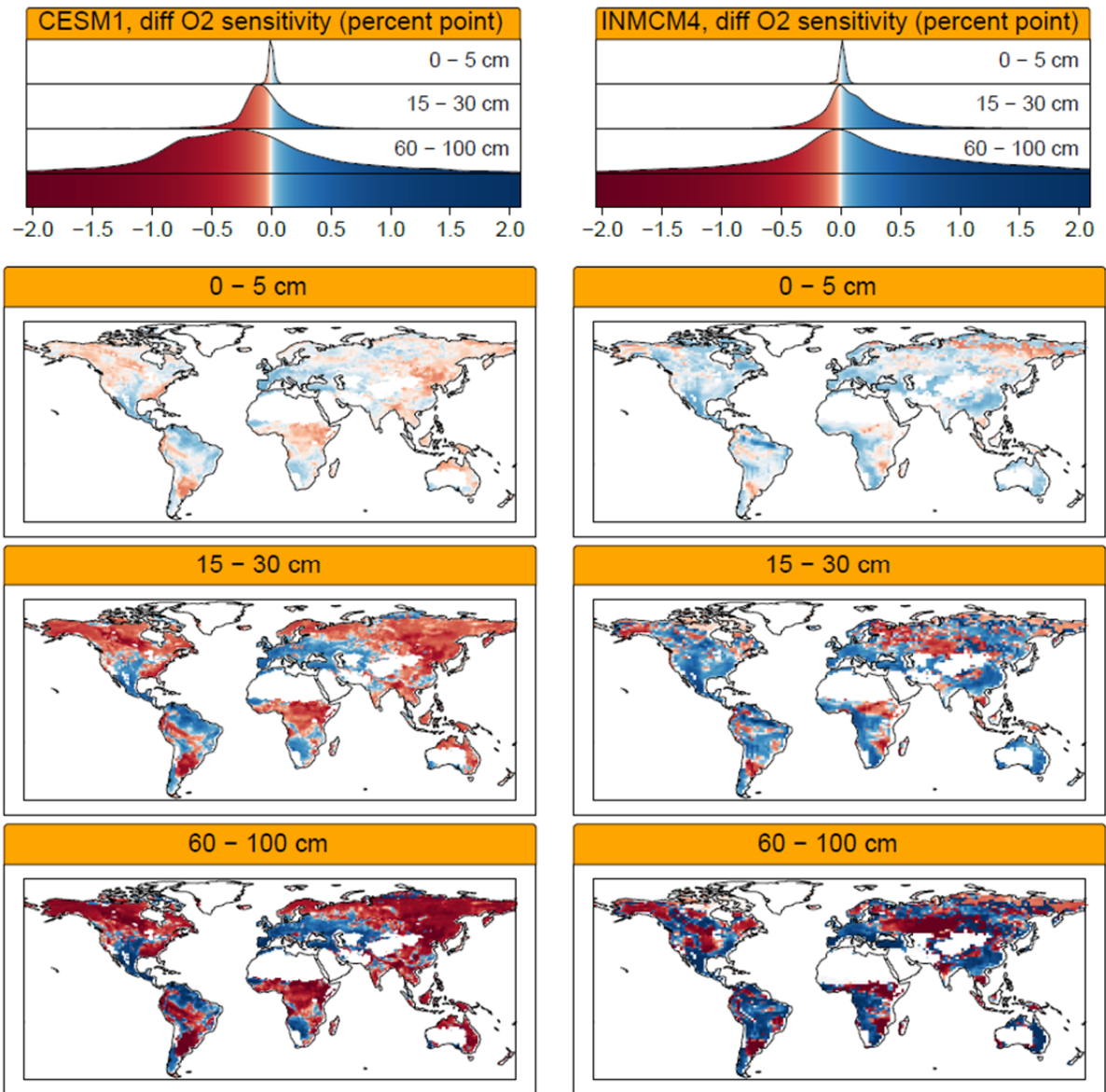


Figure S8a. Comparison of 'SM only' results between a model run with constant $O_{2,airfrac}$ (at 0.21) and a run with linear oxygen decline (0.21 – 0.04 between 0 – 100 cm depth). Values are in percent point for three different soil depths, for model CESM1-BGC (left panel) and INM-CM4 (right panel).

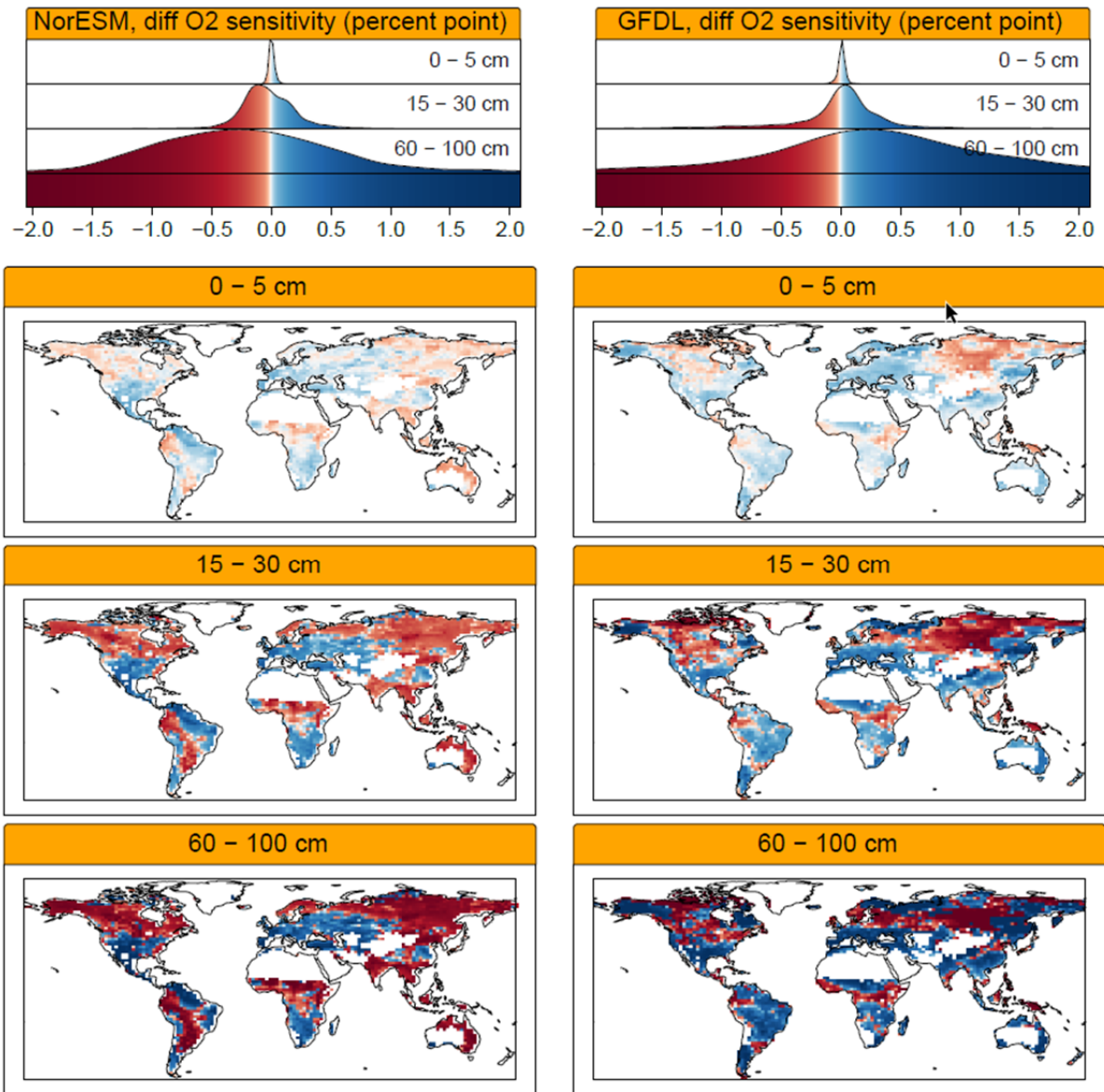


Figure S8b. Comparison of 'SM only' results between a model run with constant $O_{2,airfrac}$ (at 0.21) and a run with linear oxygen decline (0.21 – 0.04 between 0 – 100 cm depth). Values are in percent point for three different soil depths, for model NorESM-1M (left panel) and GFDL-ESM2M (right panel).

Parameter/Constant	Description	Value	Units
α_{S_x}	Base rate (pre-exponential factor)	5.38 E ¹⁰	mg C cm ⁻³ soil h ⁻¹
Ea_{S_x}	Activation energy for substrate	72.76	kJ mol ⁻¹
R	Universal gas constant	8.314	kJ K ⁻¹ mol ⁻¹
T_{ref}	Reference temperature	283.15	K
kM_{S_x}	Michaelis constant for C substrate	9.95 E ⁻⁷	g C cm ⁻³ soil
p_{S_x}	Fraction of C substrate which is soluble	4.14 E ⁻⁴	
D_{liq}	Diffusion coefficient of C substrate in liquid phase	3.17	
kM_{O_2}	Michaelis constant for oxygen	0.121	cm ⁻³ O ₂ cm ⁻³ air
D_{gas}	Diffusion coefficient for oxygen in air	1.67	
$O_{2,airfrac}$	Fraction of oxygen in air	0.209	L O ₂ L ⁻¹ air

Table S1. Parameter values and constants used in this study. Values are identical to Davidson et al. (2012) except for T_{ref} , following Wang et al. (2012).

Model name	Model Centre or Model Groups	Number of soil layers	Spatial resolution	\overline{ST}	$\Delta\overline{ST}$	\overline{SM}	$\Delta\overline{SM}$
CESM1-BGC	Community Earth System Model Contributors	7	192 x 228	284.6 ± 10.7	3.7 ± 1.0	0.27 ± 0.08	0.0017 ± 0.01
INM-CM4	Institute for Numerical Mathematics	13	120 x 180	280.8 ± 10.4	2.8 ± 1.1	0.29 ± 0.08	-0.006 ± 0.01
NorESM-1M	Norwegian Climate Centre	7	96 x 144	283.3 ± 11.3	4.2 ± 1.6	0.27 ± 0.07	0.0005 ± 0.01
GFDL-ESM2M	NOAA Geophysical Fluid Dynamics Laboratory	10	90 x 144	282.0 ± 13.3	3.7 ± 1.2	0.24 ± 0.08	-0.002 ± 0.02

Table S2. CMIP5 models used in this study. Models were selected for their availability of layered soil moisture (mrlsl) and soil temperature (tsl) data, and their vertical resolution in the first meter (≥ 5 soil layers). \overline{ST} and \overline{SM} are the global mean soil temperature and soil moisture values predicted for the historical simulation period (1976 – 2005). $\Delta\overline{ST}$ and $\Delta\overline{SM}$ are the predicted mean soil temperature and soil moisture changes between the RCP8.5 (2070 – 2099) and historical simulation period.

References

- Davidson, E., Sudeep, S., Samantha, S. C., & Savage, K. (2012). The Dual Arrhenius and Michaelis–Menten kinetics model for decomposition of soil organic matter at hourly to seasonal time scales. *Global Change Biology*, 18(1), 371-384. doi:doi:10.1111/j.1365-2486.2011.02546.x
- Gomez, A., Powers, R. F., Singer, M. J., & Horwath, W. R. (2002). Soil Compaction Effects on Growth of Young Ponderosa Pine Following Litter Removal in California's Sierra Nevada. *Soil Science Society of America Journal*, 66(4), 1334-1343. doi:https://doi.org/10.2136/sssaj2002.1334
- Hicks Pries, C. E., Castanha, C., Porras, R., & Torn, M. S. (2017). The whole-soil carbon flux in response to warming. *Science*, eaal1319. doi:10.1126/science.aal1319
- Hu, S.-C., & Linnartz, N. E. (1972). Variations in oxygen content of forest soils undermature loblolly pine stands. Retrieved from Louisiana State University: <http://digitalcommons.lsu.edu/agexp/105>
- Runkles, J. R. (1956). Diffusion, sorption and depth distribution of oxygen in soils. (Doctor of Philosophy). Iowa State College, Digital Repository @ Iowa State University, <http://lib.dr.iastate.edu/>. Retrieved from <https://lib.dr.iastate.edu/rtd/15232> (15232)
- Silver, W. L., Lugo, A. E., & Keller, M. (1999). Soil oxygen availability and biogeochemistry along rainfall and topographic gradients in upland wet tropical forest soils. *Biogeochemistry*, 44(3), 301-328. doi:10.1007/BF00996995
- Wang, G., Post, W. M., Mayes, M. A., Frerichs, J. T., & Sindhu, J. (2012). Parameter estimation for models of ligninolytic and cellulolytic enzyme kinetics. *Soil Biology and Biochemistry*, 48, 28-38. doi:10.1016/j.soilbio.2012.01.011